2013 21st Mediterranean Conference on Control & Automation (MED)
Platanias-Chania, Crete, Greece, June 25-28, 2013

Gravity and Inclination Effects on the Design of Quadruped Robots for Space Exploration

Ioannis Kontolatis, *Student Member, IEEE*, and Evangelos Papadopoulos, *Senior Member, IEEE*

***Abstract*— Leg uncompressed length and compliance have significant impact on the performance of quadruped robots. Also, gravity has a direct effect on robot motion characteristics. This paper presents results obtained using a planar lumped parameter model of a quadruped robot and an extensive research scheme to determine the optimum design parameters for quadrupeds moving in various gravity environments. An optimum region of leg spring constant and uncompressed length emerges for level terrain traversal. The maximum values for negative and positive slopes according to forward velocity in three gravity environments are also determined. Experiments with the NTUA Quadruped are conducted to validate the simulation environment. Experimental results obtained using internal sensors show that the quadruped robot performs gaits with the desired characteristics and in accordance to simulations.**

I. Introduction

Celestial body surface exploration using robotic systems aims at answering critical scientific questions, e.g. geologic evolution, evidence of life, or gathering of valuable information for future manned missions, e.g. potential landing sites. These environments are highly unstructured and their terrain morphology changes over a few meters. Although rovers succeed in traversing level terrains with obstacles of certain size, their performance is questionable in sloped terrains and thus areas of great scientific importance are beyond their safe reach.

An alternative to wheeled robotic explorers is legged locomotion, such as the one in Fig. 1. Engineers have already acknowledged the potential advantages of such systems for planetary exploration and presented concept designs that address technical issues. To name a few, researchers at JPL proposed the ATHLETE concept, a six-limbed hybrid mobile platform designed to traverse terrain using its wheels or limbs [1]. Another six-legged robot proposed for planetary exploration is the DLR Crawler [2], an actively compliant walking robot that implements a walking layer with a simple tripod and a more complex biologically inspired gait. The robot ASTRO, part of an emulation testbed for asteroid exploration, is a six-limbed ambulatory locomotion system that replicates walking gaits of the arachnid insects to avoid surface ejection [3]. Researchers from ASL/ ETH proposed a quadruped concept design for planetary exploration that was built for upright walking. Its wide range of motion in all joints allows a crawling gait in the presence of loose soil or steep slopes, and recovery manoeuvers after tipping over [4].

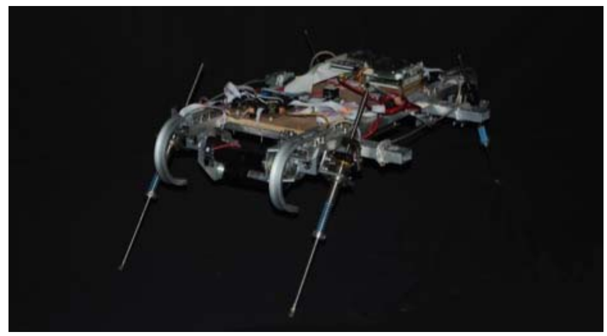

Figure 1. The NTUA Quadruped robot.

In addition, a number of approaches aiming at quadruped robots capable of sloping ground locomotion have been presented up to date. A normalized energy stability criterion presented in [5] was used as a tool to design the "intermittent crawl gait". A gait planner for generating appropriate trajectories of the body handling concave and convex slopes has been proposed in [6]. DFKI researchers presented the SpaceClimber, a biologically inspired six-legged robot for steep slopes, and focused on the foot-design of the robot aiming at handling constraints from the environmental ground conditions [7]. In [8], it was discussed how the limb length affects joint torque requirements when a gorilla-like robot is walking on a slope. Boston Dynamics' BigDog has performed well in open-field experiments in rough, sloped terrain with its forward velocity controllable using four hydraulic actuators for each leg [9]. Also, the RHex-class robots have proved their capabilities negotiating natural rough terrains [10].

The above robots perform statically stable gaits for the sake of overall motion stability and rough terrain handling, which reduces their speed capability. Also, most of them use six legs and/ or a large number of actuators. On the other hand, mission time is valuable and a reduction in travel time between targets is a clear benefit. Moreover, energy efficiency is a critical parameter for space missions. A legged robot that exploits dynamically stable gaits using the minimum number of actuators can achieve higher velocities and at the same time consume less energy. On the other hand, it is subject to complex motion control challenges and balance-in-motion constraints.

Part of this research has been co-financed by the European Union (European Social Fund – ESF) and Greek national funds through the Operational Program "Education and Lifelong Learning" of the National Strategic Reference Framework (NSRF) – Research Funding Program: THALES: Reinforcement of the interdisciplinary and/or inter-institutional research and innovation.

I. Kontolatis, and E. Papadopoulos are with the Department of Mechanical Engineering, National Technical University of Athens, 15780, Athens, Greece, (e-mail: {ikontol; egpapado}@central.ntua.gr).

In this paper, we use a planar lumped parameter model of a quadruped robot and an extensive search scheme to determine the optimum region of the design parameters for a quadruped moving in three different gravity environments. First, the optimum region of leg spring constant and uncompressed length is determined for level terrain traversal. Next, the maximum values for negative and positive slopes according to forward velocity in the three gravity environments are defined. We use the NTUA Quadruped (Fig. 1) to conduct experiments in Earth's gravity and evaluate the effect of leg stiffness upon motion parameters, i.e. forward velocity and body pitch. Experimental results obtained using internal sensors show that the quadruped robot performs gaits with the desired characteristics.

I. Quadruped Robot Dynamics

A. Robot Model

Fig. 2 shows a lumped parameter physical model of the quadruped robot employed in this paper. The model consists of two compliant virtual legs (VLegs) of mass m_j and uncompressed length l_{0j}, and a body of mass m_b and inertia I_b respectively. The index j indicates a rear (r) or a front (f) VLeg. A VLeg, front or rear, models the two respective physical legs that operate in pairs when a gait is realized and exerts equal torques and forces on the body as the set of the two physical ones [11].

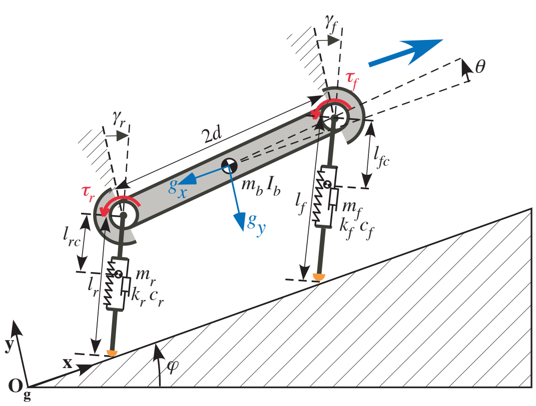

Figure 2. A lumped parameter planar quadruped model.

Each VLeg is connected to the main body with an actuated rotational joint at distance d from the body center of mass (CM). This body can rotate by an angle θ around the z-axis and thus the model captures the body pitch stabilization problem. The rotational hip joint allows for positioning of VLegs at angle γ_j in the sagittal plane. Also, each VLeg has a passive prismatic joint modeled as a linear compression spring of constant k_j and viscous damping coefficient c_j. The prismatic joint allows changes of the VLeg length l_j and energy accumulation during locomotion. Table I summarizes robot and motion parameters.

B. Motion Phases and Transitions

A quadruped robot, studied in the sagittal plane, goes through four phases of the three-link (rear VLeg, front VLeg, main body) kinematic chain, i.e. double stance, flight, front stance, rear stance, as presented in Fig. 3. The realization of the gait depends on which legs are working in pairs, which motion phases appear and for how long, the values of the leg touchdown angles and body pitch angle.

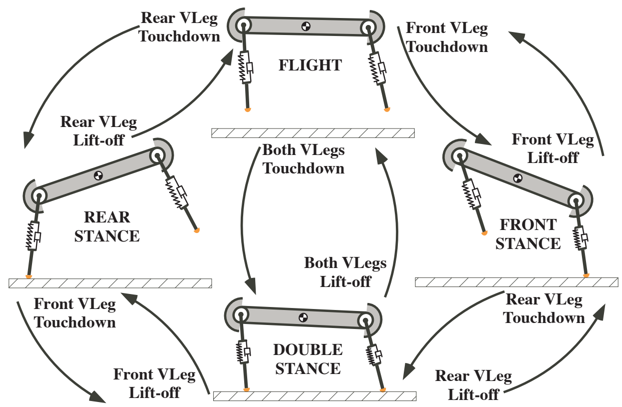

Figure 3. Motion phases and events that trigger them.

Pronking is the gait when all legs are, either in contact with the ground (double stance) or not (flight). The bounding gait has two additional intermediate phases, namely the ones in which only one set of legs (rear or front) is in contact with the ground. In pronking, zero or close to zero pitching is expected. However, in the non-ideal case, where body pitching occurs, the rear or front legs may strike the ground first. Then, pronking reduces to bounding.

TABLE I. Robot and Motion Parameters

Symbol	Quantity	Symbol	Quantity
x_c	Body CM x-axis coordinate	c	VLeg viscous damping
y_c	Body CM y-axis coordinate	γ	VLeg angle w.r.t. $\mathbf{O_g xy}$
θ	Body pitch angle	m	VLeg mass
I_b	Body inertia w.r.t. z-axis	d	Hip joint to CM distance
m_b	Body mass	φ	Ground inclination
x	VLeg CM x-axis coordinate	τ	Hip torque
y	VLeg CM y-axis coordinate	r	As index: rear VLeg
l	VLeg length	f	As index: front VLeg
l_0	VLeg uncompressed length	td	As index: value at touchdown
k	VLeg spring constant	lo	As index: value at liftoff

Legged robots are hybrid systems and therefore their motion cannot be described by a single set of equations. A set of continuous equations for each phase together with discrete transformations governing transitions from one phase to the next are required to model the dynamics of such systems. The transition equations that determine the touchdown and lift-off events of the rear and front VLegs during plane motion are:

$$y_c + d\sin(\theta_{td}) \le l_{0f}\cos(\gamma_{f,td}) \tag{1}$$

$$l_{r,lo} = l_{0r} \tag{2}$$

$$l_{f,lo} = l_{0f} \tag{3}$$

Eqs. (1) and (2) describe the conditions of touchdown events, while (3) and (4) describe the conditions of liftoff events. Which event will occur depends on length comparison; Table II summarizes which event trigger equations correspond to each phase.

TABLE II. PHASE TRANSITION EQUATIONS

Motion Phase	*Transition Equations #*
Flight	(1), (2)
Rear Stance	(2), (3)
Double Stance	(3), (4)
Front Stance	(1), (4)

C. Equations of Motion

The robot motion is studied in the sagittal plane. During the flight phase (both VLegs do not touch the ground), the robot's CM performs a ballistic motion with constant system angular momentum with respect to the CM. During stance phase, the VLeg(s) that are in contact with the ground move the body forward. The equations of motion for the main phases, i.e. flight (*FL*) and double stance (*ST*), and for the intermediate ones, i.e. front (*FST*) and rear stance (*RST*), are derived using a Lagrangian formulation. During double stance phase the vector of the generalized coordinates is

$$\mathbf{q}_{ST} = \begin{bmatrix} x_c & y_c & \theta & \gamma_r & \gamma_f \end{bmatrix}^T \tag{4}$$

and the Lagrangian of the robot is:

$$\begin{aligned} L_{RobotST} &= L_{BodyST} + L_{VLegrST} + L_{VLegfST} = \\ &\frac{1}{2}m_b(\dot{x}_c^2 + \dot{y}_c^2) + \frac{1}{2}I_b\dot{\theta}^2 - m_b g_x x_c - m_b g_y y_c \\ &+ \frac{1}{2}m_r(\dot{x}_r^2 + \dot{y}_r^2) - \frac{1}{2}k_r(l_{0r} - l_r)^2 - m_r g_x x_r - m_r g_y y_r \\ &+ \frac{1}{2}m_f(\dot{x}_f^2 + \dot{y}_f^2) - \frac{1}{2}k_f(l_{0f} - l_f)^2 - m_f g_x x_f - m_f g_y y_f \end{aligned} \tag{5}$$

The ground inclination, positive or negative, affects robot dynamics through the two gravity components g_x, g_y:

$$g_x = g \cdot \sin(\varphi), \qquad g_y = g \cdot \cos(\varphi) \tag{6}$$

Rear (x_r, y_r) and front (x_f, y_f) VLeg CM coordinates can be expressed as functions of the generalized coordinates using geometrical relationships:

$$\begin{aligned} x_r &= x_c - d\cos(\theta) + l_{rc}\sin(\gamma_r) \\ y_r &= y_c - d\sin(\theta) - l_{rc}\cos(\gamma_r) \end{aligned} \tag{7}$$

$$\begin{aligned} x_f &= x_c + d\cos(\theta) + l_{fc}\sin(\gamma_f) \\ y_f &= y_c + d\sin(\theta) - l_{fc}\cos(\gamma_f) \end{aligned} \tag{8}$$

The energy dissipation due to prismatic joint viscous damping is:

$$P_{Diss} = \frac{1}{2}c_r\dot{l}_r^2 + \frac{1}{2}c_f\dot{l}_f^2 \tag{9}$$

The energy contribution of actuator torques is given by:

$$P_{Contr} = \tau_r(\dot{\gamma}_r - \dot{\theta}) + \tau_f(\dot{\gamma}_f - \dot{\theta}) \tag{10}$$

Variables l_r, γ_r, l_f, γ_f are derived using kinematic relationships:

$$l_r = \sqrt{(x_{tr,td} + d\cos(\theta) - x_c)^2 + (d\sin(\theta) - y_c)^2} \tag{11}$$

$$\gamma_r = A\text{rctan}(-d\sin(\theta) + y_c, x_{tr,td} + d\cos(\theta) - x_c) \tag{12}$$

$$l_f = \sqrt{(x_{tf,td} - d\cos(\theta) - x_c)^2 + (d\sin(\theta) - y_c)^2} \tag{13}$$

$$\gamma_f = A\text{rctan}(d\sin(\theta) + y_c, x_{tf,td} - d\cos(\theta) - x_c) \tag{14}$$

Rear $x_{tr,td}$ and front $x_{tf,td}$ toe location are given by:

$$x_{tr,td} = x_c + l_r\sin(\gamma_r) - d\cos(\theta) \tag{15}$$

$$x_{tf,td} = x_c + l_f\sin(\gamma_f) + d\cos(\theta) \tag{16}$$

when touchdown occurs without toe slippage.

During the flight phase the generalized coordinates vector is the same as (5) and the Lagrangian of the robot is (6) with the spring terms omitted, while there is no energy dissipation and contribution. For the two intermediate phases, i.e. rear and front stance, vector $\mathbf{q}_i$ does not include l_r, γ_r or l_f, γ_f respectively, which are calculated again by (12), (13) and (14), (15), and the Lagrangian, energy dissipation and contribution equations of each phase miss the appropriate terms. Equations of motion for all phases are derived as [12]:

$$\frac{d}{dt}\left(\frac{\partial L_{Robot,i}}{\partial \dot{\mathbf{q}}_i}\right)^T - \left(\frac{\partial L_{Robot,i}}{\partial \mathbf{q}_i}\right)^T + \left(\frac{\partial P_{Diss,i}}{\partial \dot{\mathbf{q}}_i}\right)^T - \left(\frac{\partial P_{Contr,i}}{\partial \dot{\mathbf{q}}_i}\right)^T = \mathbf{0} \tag{17}$$

where *i* is the phase index, i.e. *ST*, *FL*, *RST*, *FST*.

II. DESIGN PARAMETER ANALYSIS

Leg uncompressed length l_0 and stiffness k have a significant impact on the dynamically stable quadruped robot performance, i.e. maximum achievable velocity and maximum ground slope handling, and efficiency, i.e. actuator torque requirements. In addition, the gravity has a direct effect on robot's motion. A question that rises, considering a celestial body surface exploration mission, is which are the optimum values for the design parameters l_0 and k subjected to criteria, such as energy efficiency and motion stability.

To answer this question, we use the quadruped robot model presented in Section II to perform an extensive search through the set of possible solutions. Due to energy dissipation and to make a repeatable motion achievable, a controller must be able to maintain the system energy level. The multi-part controller presented in [13] is used because it allows forward velocity and apex height to be set and maintained at desired values, while keeps body pitch rate close to zero for stability. Therefore, this controller allows the robot to traverse uneven terrains with a desired velocity. Also, it can be applied to a robot with only one actuator per leg thus enhances energy efficiency.

The extensive search scheme used in this work was set using the Matlab environment and has a two-layer structure. The inner layer involves the robot motion simulation. The equations of motion of each phase presented in Section II are solved using the ODE45 function and which set of them is solved each time is determined by the transition equations

(1)-(4). The multipart controller function calculates during each flight phase the leg touchdown angles and actuator torques for the upcoming stance phase (rear, double or front). A simple PD-controller is used to position legs to the calculated desired touchdown angles. The robot motion simulation was set to be terminated when the robot had completed 100 strides, i.e. complete cycles considered from a reference limb, e.g. rear left, flight phase till the next.

The outer layer involves definition of the initial conditions, the quadruped model physical parameters, the environment parameters and the desired motion parameters. This definition is programmed as a loop function to make the extensive search through a range of values of the parameters of interest feasible. In this work, parameters of interest include uncompressed leg length and stiffness, gravity and ground inclination, quadruped forward velocity, while Table III displays the parameter values that kept constant during the extensive search scheme.

TABLE III. CONSTANT PARAMETERS DURING SIMULATIONS

Parameter	*Value*
Initial robot CM vertical position	0.35 m
Initial body pitch	0 rad
Initial body pitch rate	0.5 rad/ s
Initial vertical velocity	0 m/ s
Initial forward velocity	0.4 m /s
Body mass	9 kg
VLeg mass	0.62 kg
Hip joint viscous friction coefficient	0 Nms/ rad
Prismatic joints viscous friction coefficient	10 Ns/ m
Hip joint distance	0.50 m
Body inertia	0.5625 kgm^2
Desired robot CM apex height	0.32 m

To study the effects of gravity, Earth, Mars and Moon-like gravity environments were selected. The extensive search for possible solutions was conducted for level and sloped ground on the three gravity environments.

A. *Level Terrain*

First, we seek to find the range of VLeg spring constant that makes desired forward velocities achievable and these maximum achievable forward velocities for each gravity environment. We use the extensive search scheme with a forward velocity range 0.3 to 2.0 m/s and 0.1 m/s step size and VLeg spring constant range 100 to 20000 N/m and step size 100 N/m. In addition to Table III parameters, uncompressed leg length and ground inclination are kept constant, at 0.30 m and 0 deg respectively. The results considering spring constant vs. forward velocity for the three gravity environments are presented in Fig. 4 and will be discussed later.

Next, we seek to find the range of uncompressed leg length. Forward velocity range and step size are the same as previously, while uncompressed leg length range is 0.20 to 0.60 m and step size is 0.01 m. In this case VLeg spring constant is not a parameter of interest and is altered only when gravity changes according to the first search scheme results. Thus, additionally to Table III parameters, ground inclination of 0 deg and VLeg spring stiffness of 6000 N/m (Earth), 3000 N/m (Mars) and 1800 N/m (Moon) are kept constant. The results considering uncompressed leg length vs. forward velocity are presented in Fig. 5.

Both Fig. 4 and Fig. 5 show that regions for every environment can be identified that make achievable different values of forward velocity. As gravity is reduced, the springs need to be softer to accumulate energy more efficiently while legs can be longer. Also, the maximum achievable forward velocity becomes lower as gravity drops. It can be observed that for a given forward velocity, e.g. 1 m/s, a range of VLeg spring constants, i.e. 2200 to 16900 N/m, and VLeg uncompressed lengths, i.e. 0.29 to 0.45 m exists. Although all values in these ranges make the specific forward velocity feasible, there is a tradeoff. As leg springs become stiffer, torque requirements increase (Fig. 6, blue line). On other hand, softer springs lead to larger variations of body pitch (Fig. 7).

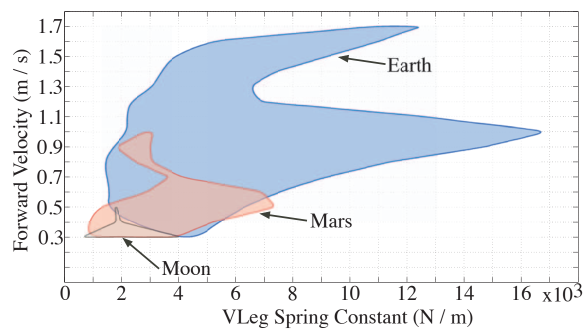

Figure 4. Spring constant vs. fwd velocity. Level terrain.

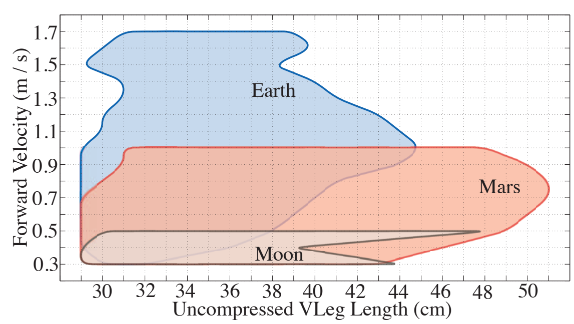

Figure 5. Uncompressed leg length vs. fwd velocity. Level terrain.

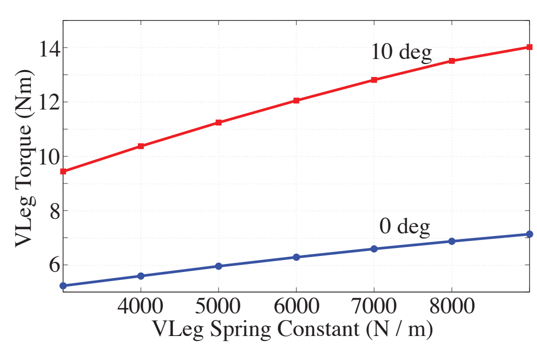

Figure 6. Actuator torque requirements for different VLeg spring constant. Level and slopped terrain.

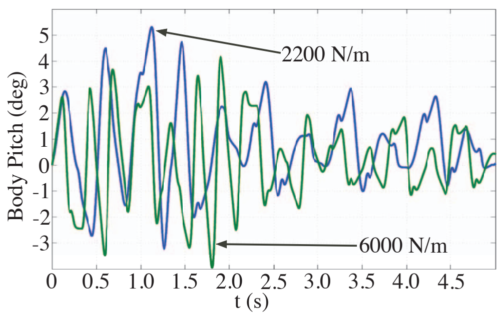

Figure 7. Body pitch for 2200 and 6000 N/m VLeg spring constant.

B. Sloped Terrain

In the case of sloped terrains, we seek the maximum values of positive and negative slopes as a function of forward velocity in the three gravity environments. We use the extensive search scheme with forward velocity range 0.3 to 2.0 m/s and 0.1 m/s step size and ground inclination range -30 to 30 deg and step size of 1 deg. In addition to Table III parameters, the uncompressed leg length and VLeg spring stiffness are kept constant. The uncompressed leg length is 0.30 m for all gravity environments and the spring stiffness is 6000 N/m (Earth), 3000 N/m (Mars) and 1800 N/m (Moon). The results are presented in Fig. 8. In all cases, the robot handles steeper slopes with reduced velocities. The maximum VLeg torque requirements for this performance are limited by 14 Nm. i.e. the limit for the DC motors used in the NTUA Quadruped.

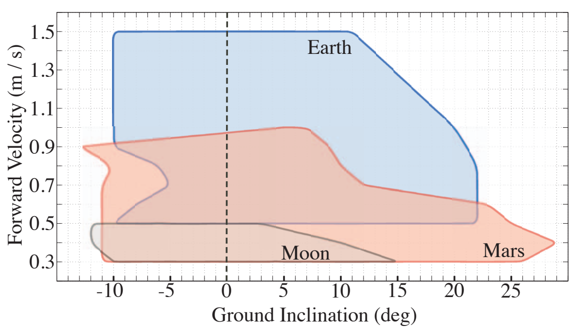

Figure 8. Achievable forward velocity vs. ground inclination for different gravity environments (Earth, Mars, Moon).

III. NTUA Quadruped Experiments

A. Hardware Description

The NTUA Quadruped (Fig. 1) has legs with springs and only one actuator per each hip joint. The total mass of the robot is 11 kg, including motors, gearboxes, sensors, electronics, LiPo batteries and onboard computer. All robot design parameters have been selected using a systematic methodology and are optimal according to selected performance criteria [14]. These criteria are (a) minimization of energy requirements to sustain a certain motion and (b) maximization of payload capability for the target robot mass. Table IV summarizes the NTUA Quadruped physical parameters.

The chassis is made of aluminum and is modular, i.e. the body length, width, weight distribution and symmetry are adjustable. The legs are made of steel, for durability against impact forces, and consist of two main parts, i.e. upper and lower, and a spring coil to form a compliant prismatic joint, presented in Fig. 9(a). The lower part slides into the upper. The design of the leg allows adjustments in the leg uncompressed length and the spring pre-tension. The legs' uncompressed length can be adjusted to a maximum of about 25% of the average leg length. In addition, the spring can be replaced easily to adjust leg compliance. The toes are made of shock absorbing material, which also keeps friction between the ground and the leg toes high. An electric motor actuates each hip joint and places each leg to the desired angle, using a pulley-belt mechanism. Four full quadrature encoders fitted on each motor are used for leg angle measurements. Another four encoders incorporated in a 2-link mechanism, which transforms linear displacement to rotational, are used to measure spring compression (Fig. 9(b)). A six dof inertial measurement unit (IMU) is mounted on the robot at its CM. IMU measurements are used for monitoring, but also for feeding back the pitch angle. Table V displays information regarding the NTUA Quadruped main components.

(a) (b)

Figure 9. (a) Leg showing compliant spring and angle range, and (b) leg length measurement mechanism design.

TABLE IV. NTUA Quadruped Physical Parameters

Parameter	*Value*
Robot mass	11.00 kg
Leg uncompressed length	0.25 – 0.38 m
Spring stiffness	1000 – 6000 N/ m
Hip joint distance	0.54 m
Body inertia	2.917 kg m^2

TABLE V. NTUA Quadruped Main Components

Component	*Specifications*
Actuators	4 Maxon RE30 60W DC, 0.85 Nm
Amplifiers	4 AMC DZRALTE-012L080
Encoders	4 Avago HEDS-5540, 3Ch, 500 cpr (leg angle)
	4 US Digital E4P, 2Ch, 360 cpr (leg compression)
IMU	1 Analog Devices ADIS 16354
Onboard PC	1 PC/104 256MB 650Hz
MCU	8 dsPIC 30F4012 (encoder reading)
	2 ATMEL ATMEGA16 (IMU, dsPICs, PC/104)
Power Supply	Li-Po battery packs

B. Experiments

The experiments conducted with the NTUA Quadruped robot on level ground and Earth gravity. The robot multipart controller is the same with one used in the simulations. In each experiment, the robot is released from an initial height of approximately 0.05m above the ground. This way of starting is necessary for achieving an initial spring compression, and thus energy accumulation. The robot continues its periodical motion through the separate phases that characterize each gait and described in Section II. The basic goal of these experiments is to validate the simulation environment. If the NTUA Quadruped with a specific combination of leg stiffness and uncompressed length performs similarly with the simulated model on Earth gravity, we can safely assume that the simulation environment results for other planets are valid.

The multipart controller guides the quadruped robot to realize gaits with desired forward velocity between 0.8 to 1.0 m/s and apex height around 0.29 – 0.32 m depending on leg uncompressed length. The body pitch rate is kept around 0 deg/s. Fig. 10 and 11 present the body pitch and the forward velocity data from the IMU sensor in comparison with results from simulation for the first 5 seconds of robot motion. After these 5 seconds, the robot repeats its gait. It can be seen that although a simple model was employed in the simulation studies, response results are close to the experimental ones. Additional experiments are planned using the lab's speed-controlled and adjustable inclination treadmill.

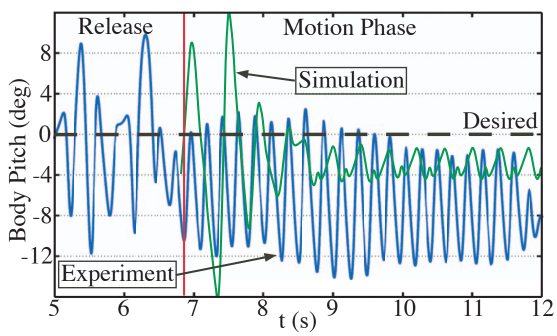

Figure 10. Body pitch. Simulation and IMU data. Level terrain.

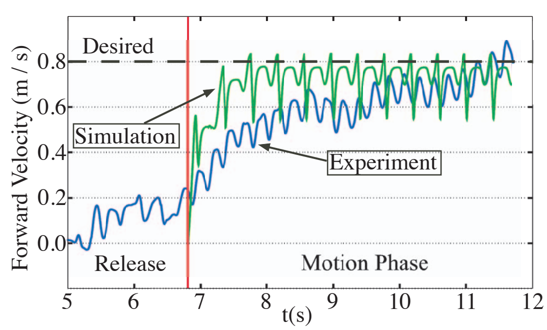

Figure 11. Forward velocity. Simulation and IMU data. Level terrain.

IV. Conclusions

In this paper, a planar lumped parameter model of a quadruped robot and an extensive research scheme were used to determine the optimum design parameters for a quadruped moving in different gravity environments, i.e. Earth, Mars and the Moon. First, optimum values for leg spring constants and uncompressed lengths were determined for level terrain. Next, the maximum values of negative and positive slopes according to forward velocity as a function of gravity were defined. The results showed that for every environment an optimum region of design parameters can be identified that allows for different values of forward velocity. It was found that as gravity drops, the leg springs need to be softer to accumulate energy. Moreover, the maximum achievable forward velocity is lower in Mars and even lower in the Moon. In addition, as leg springs become stiffer, torque requirements increase. However, the use of softer springs leads to larger variations of the robot body pitch.

The NTUA Quadruped was also used to conduct experiments on level terrain on Earth. Experimental results obtained using internal sensors showed that the quadruped performs gaits with the desired characteristics. In addition, robot performance with specific leg stiffness and uncompressed length was similar to the simulated model with the same parameters.

References

[1] Heverly, M. and Matthews, J., "A Wheel-on-limb rover for lunar operation," *Proc. Inter. Symposium on Artificial Intelligence, Robotics and Automation in Space(i-SAIRAS)*, Hollywood, USA, 2008.

[2] Görner, M., Chilian, A. and Hirschmüller, H., "Towards an Autonomous Walking Robot for Planetary Surfaces," *Proc. International Symposium on Artificial Intelligence, Robotics and Automation in Space (i-SAIRAS)*, Sapporo, Japan, 2010.

[3] Chacin, M. and Yoshida, K., "A Microgravity Emulation Testbed for Asteroid Exploration Robots," *Proc. International Symposium on Artificial Intelligence, Robotics and Automation in Space (i-SAIRAS)*, Hollywood, USA, 2008.

[4] Latta, M., Remy, C. D., Hutter, M., Höpflinger, M. and Siegwart, R., "Towards Walking on Mars," *Proc. Symp. Advanced Space Technology in Robotics & Automation*, ASTRA, Noordwijk, Netherlands, 2011.

[5] Hirose, S., H. Tsukagoshi, and K. Yoneda, "Normalized Energy Stability Margin and its Contour of Walking Vehicles on Rough Terrain," in *Proc. IEEE International Conference on Robotics and Automation (ICRA)*, Seoul, Korea, 2001, pp. 181-186.

[6] H. Kim, T. Kang, V. G. Loc, and H. R. Choi, "Gait Planning of Quadruped Walking and Climbing Robot for Locomotion in 3D Environment," in *Proc. IEEE International Conference on Robotics and Automation (ICRA)*, Barcelona, Spain, 2005, pp. 2733 – 2738.

[7] Bartsch, S. et al., "SpaceClimber: Develop-ment of a Six-Legged Climbing Robot for Space Exploration," *Proc. ISR/ROBOTIK*, Munich, Germany, 2010.

[8] Aoyama, T., K. Sekiyama, Y. Hasegawa, and T. Fukuda, "Analysis of Relationship between Limb Length and Joint Load in Quadruped Walking on the Slope," *Proc. IEEE/ RSJ Int. Conference on Intelligent Robots and Systems (IROS)*, Nice, France, 2008, pp. 3908-3913.

[9] Raibert, M., "BigDog, the Rough-Terrain Quadruped Robot," *Proc. IFAC World Congress,* South Korea, 2008.

[10] Saranli, U., Buehler, M., Koditschek, D.E. "Rhex - a simple and highly mobile hexapod robot," *International Journal of Robotics Research* 20(7), 2001, pp. 616-631.

[11] Raibert, M. *Legged Robots That Balance*, MIT Press, Cambridge, MA, 1986, pp. 92-95.

[12] Siciliano, B., Sciavicco, L., Villani, L., Oriolo, G. *Robotics. Modeling, Planning and Control*, Springer-Verlag, London, 2010, pp. 247-257.

[13] Cherouvim, N., Papadopoulos, E. Novel Energy Transfer Mechanism in a Running Quadruped Robot with One Actuator per Leg. *Advanced Robotics*, 24(7), 2010, pp. 963-978.

[14] Chatzakos, P., Papadopoulos, E., "Bio-inspired Design of Electrically-Driven Bounding Quadrupeds via Parametric Analysis," *Mechanisms and Machine Theory*, 44(3), 2010, pp. 559-579.